From Nanoelectronics to Nano-Spintronics

Kang L. Wang*, Igor Ovchinnikov, Faxian Xiu, Alex Khitun, and Ming Bao

*Device Research Laboratory (DRL), Marco Focus Center on Functional Engineered Nano Architectonics—FENA,
Western Institute of Nanoelectronics—WIN, California NanoSystems Institute—CNSI, University of California,
Los Angeles, CA 90095-1594, USA*

Today's electronics uses electron charge as a state variable for logic and computing operation, which is often represented as voltage or current. In this representation of state variable, carriers in electronic devices behave independently even to a few and single electron cases. As the scaling continues to reduce the physical feature size and to increase the functional throughput, two most outstanding limitations and major challenges, among others, are power dissipation and variability as identified by ITRS. This paper presents the exposé, in that collective phenomena, e.g., spintronics using appropriate order parameters of magnetic moment as a state variable may be considered favorably for a new room-temperature information processing paradigm. A comparison between electronics and spintronics in terms of variability, quantum and thermal fluctuations will be presented. It shows that the benefits of the scalability to smaller sizes in the case of spintronics (nanomagnetics) include a much reduced variability problem as compared with today's electronics. In addition, another advantage of using nanomagnets is the possibility of constructing nonvolatile logics, which allow for immense power savings during system standby. However, most of devices with magnetic moment usually use current to drive the devices and consequently, power dissipation is a major issue. We will discuss approaches of using electric-field control of ferromagnetism in dilute magnetic semiconductor (DMS) and metallic ferromagnetic materials. With the DMSs, carrier-mediated transition from paramagnetic to ferromagnetic phases make possible to have devices work very much like field effect transistor, plus the non-volatility afforded by ferromagnetism. Then we will describe new possibilities of the use of electric field for metallic materials and devices: Spin wave devices with multiferroics materials. We will also further describe a potential new method of electric field control of metallic ferromagnetism via field effect of the Thomas Fermi surface layer.

Keywords: Nanoelectronics, Spintronics, Dilute Magnetic Semiconductors, Spin Wave, Field Controlled Ferromagnetism.

1. INTRODUCTION

Nanoscience and nanotechnology arise due to the interest of scaling to atomic scale from the macroscopic world. On the other hand, we may fundamentally look at subjects by zooming out the length-scale from elementary particles to atoms, molecules, and crystals, etc. The physical systems and phenomena start acquiring distinctive properties and features, well-known from our every-day experience of the macroscopic world. At the atomic size, it is the very electromagnetic interaction between the electrons and the positively charged nuclei, which determine all the properties as characterized by a set of order parameters or collective variables. When the engineering the feature sizes down to nanometers, we arrive at this new identification of nanoscience and nanotechnology, which take its origin not from what the physical phenomenon under consideration looks like, but from the scale that the parental (electromagnetic) interactions dominates. But from the physics point of view, it is the very electromagnetic interactions between the electrons and the positively charged nuclei, which determine all the properties as characterized by a set of order parameters or collective variables.

For continuing the miniaturization trend, there has been increasing interest in considering room temperature collective phenomena (fields) as an alternate to scaled CMOS for next generations of information processing beyond today's electronics. In the past, scaled CMOS, electron charge and its representations e.g., voltage and current, are used as a state variable for device to perform logic functions. Upon further scaling to the nanometer scale, the use of electron charge and its increasingly strong long-range Coulomb interactions resulted in two major problems: power dissipation per unit area and variability of the device. The first

*Author to whom correspondence should be addressed.

comes from the strong Coulomb interaction. It is shown that the minimal energy of a switch is $kT \ln \gamma$ for an equilibrium system; for n electrons, the energy required will be $nkT \ln \gamma$ if electrons work independently, where n is the number of electronics and γ is the reliability factor, or reciprocal of the probability of failures. The variability problem comes from the result of independent electrons in the device; the scaling to small feature sizes makes the quantum fluctuations of electrons larger when the number of electron decreases.

In the continuing scaling of the feature size of semiconductor devices, there are two major issues for further scaling: power dissipation and variability.[1] To resolve the major challenges of power dissipation and variability issues, among others, it is necessary to introduce corrections to the Coulomb interaction. The corrections may be very roughly divided into the dynamic or relativistic (magnetic and spin-related), the static (short-range multiple poles) and the quantum or many-body (such as many body effects due to the Fermi-statistics of the electrons). At present, it is not possible to use any part of the electromagnetic interactions on a single-electron level other than Coulomb, since the strength of others is too small to afford room temperature operation as to be discussed later. One viable solution is to use the collective variables in the correlated many-electron systems for room temperature operation. The use of the collective variables, which represent many-electron systems, assumes that the variable is energetic enough to be thermally stable.

An example of using collective effects as variables is ferromagnetism in nanomagnets, e.g., MTJ junctions, in which the order parameter in this case is the magnetization of the active ferromagnetic layer (typically of a few nanometers to tens of nanometers in size) as controlled by passing through the electric current. The layer consists of tens to thousands of atoms, each of which contributes its spins to the overall collective variable—the magnetization. It is the nanometer-size of the layer, which makes it possible that the magnetization along one of the possible directions remains for a very long period of time. Additional possibilities, which can be employed to exploit the collective variables, exist, including the electric dipole polarization of an isle of the ferroelectric or multiferroic materials or even dislocations in the crystal. The latter not only can constitute as collective variables themselves, but the elementary excitations of these collective variables can also be treated as variables—the excitation of the order parameters (primary collective variables) can be themselves treated as variables. For the same class of the hierarchy of the collective excitations, one may include others such as the domain-walls and spin-waves in a ferromagnet. In this paper, we will focus on the collective ferromagnetic variable.

In spintronics, there are usually two scenarios: one is single spin case and the other the collection of interaction spins (with exchange interaction, which is the quantum correlation to the Coulomb interaction). For the former, it will be similar to that of electronics. There are advantages in energy and in variability when using collective magnetic degree of freedom, in particular, in the case that the energy associated with the variable is higher than kT for room temperature applications. The variability due to the quantum fluctuations becomes less critical in the collective spin degree of freedom (as to be discussed further next).

2. VARIABILITY OF ELECTRONICS AND SPINTRONICS

From the above discussion, spintronics[2] has emerged as a potential candidate in addition to others in search of low power and variability devices. In this section, we address the variability issue of nanoscaled electronic and spintronics devices. There are different sources of variability due to thermal and quantum fluctuations, resulted from the fluctuations of, for example, the number of electrons and process control such as pattern size and dopant variations in semiconductor FET. Let us, however, focus on the fundamental source of quantum fluctuations.[3]

In order to assess electronic and spin based circuits for their variability, one can address the problems of the importance of uncontrolled quantum fluctuations in the elemental units—FET and, without loss of generality, a magnetic gate of some variations of Spin-FET. The input-output fluctuations in a generic transistor can be understood from rather general thermodynamics reasoning. When the retardation (delay) effects are neglected, the output variable can be assumed to be in an "on-time" correspondence with the state variable of the gate (the charge Q or the magnetization M), so that $V_{\text{out}} = f(Q)$. In turn, the state variable is controlled by the input parameter (V_{in} or S_{in}), which is effectively its Legendre conjugate in a thermodynamic potential (e.g., the free energy F), governing the behavior of the system, which is thermally open to heat bath(s). The effective couplings in the thermodynamical potential are QV_{in} and $S_{\text{in}}M$. Depending on which variable is fixed, the corresponding potential must be used. Thus, just as for any Legendre conjugate pair (e.g., pressure-volume, temperature-entropy, chemical potential-number of particles), fixing one variable (the input, i.e., V_{in} and S_{in}), we leave the other variable (output, Q or M) loose and let it fluctuate—due to thermal fluctuations at high temperatures and/or due to the quantum discreteness of the state variable's eigenvalues at low temperatures. In Figure 1, we summarized the results of the analysis, based on the "minimal" Hamiltonian approach, showing the comparison of the charge and spin minimal feature sizes due to the existence of the domain of the quantum fluctuations as well as illustrating the feature size on top and the number of atoms on the bottom axis for a given device using a spherical gate, 1 2-D gate. The room
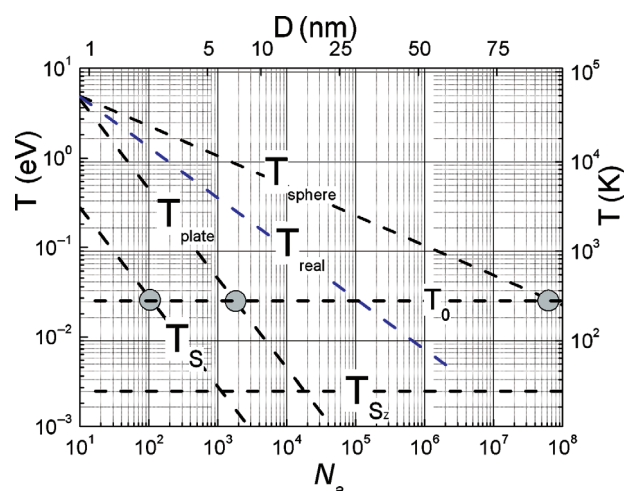
Fig. 1. Domains of quantum fluctuations for three quantum numbers: N, S, and S_z. The curves, T_{sphere}, T_S and Ts_z separate the domains of the quantum (to the left and down) and the thermal (to the right and up) fluctuations of the corresponding quantum number for a sphere gate (black dashed line). Likewise, for a 2-D plate (dashed line) and a more realistic gate (blue solid line), data are given, respectively. At 300 K, the fluctuations in the magnetic quantum number S give the limiting number of 10^2 atoms versus the electronics counterpart of $\sim 10^5$ atoms.

temperature line is also shown. Clearly, the exact geometry of the gate electrode will change the capacitance and also affect the number for the "charge" line. In addition, for realistic devices, the gate capacitance will also depend on the insulating dielectric layer and thus the results will be somewhere in between as also shown. These numbers obtained should be good on the order of the magnitude. The numbers can be plotted together with the limitation based on energy consideration discussed above. Different materials can be used and there will be different sizes as a result of using atomic sizes.

The fact that the spin degree of freedom is more advantageous than the charge degree of freedom from the quantum fluctuations point of view has its origin in the locality of the interaction responsible for the magnetism (exchange interaction). On the energy scale the energy per "quantum unit" scales as $1/r$ for electronics (Coulomb repulsion), whereas it is size independent for spins (exchange). For this paper, we only limit ourselves to electron and spin based devices. For other cases, as in molecules (or particles) and ferroelectric materials, there will, more or less, give similar geometric dependences of the scaling rules of correlated effects or many-body (collective) effects in nanoscale systems.

The electric current control of ferromagnetism has been in practice for centuries, as earlier as the use of Helmholtz coils. However, the use of current makes power dissipation an issue. Electrical field control is most desirable from the energy dissipation point of view. To date, there are two classes of materials for electrical control of ferromagnetism: Dilute magnetic semiconductors and metallic ferromagnetic materials.

3. DILUTE MAGNETIC SEMICONDUCTOR

3.1. MnGe Self-Assembled Quantum Dots by Molecular Beam Epitaxy (MBE) and Field Controlled Ferromagnetism at 50 K
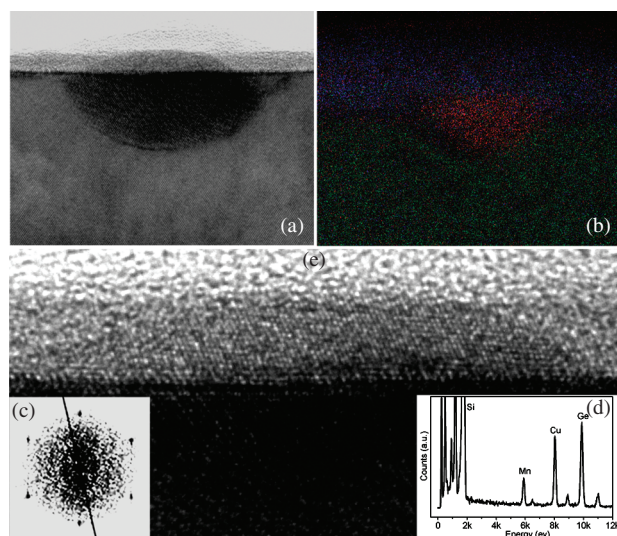
A dilute magnetic semiconductor system offers potential advantages in combining the magnetic dopants in semiconductors, making electrical field control of ferromagnetism feasible for increasing device functionalities and power dissipations.[4] It promises a new breed of magneto-electronic devices to extend the scaling of microelectronics to next generations of nanometer integrated chips for low power and low variability.[5] To understand and exploit this controllability, a number of theories have been developed in the past, including the Zener kinetic-exchange,[6] double exchange, and the Ruderman-Kittel-Kasuya-Yoshida (RKKY) interaction.[7] These models share a common feature that a spontaneous ferromagnetic order is hole-mediated through the increase of hole concentrations.[8] While precise theories involving this phenomenon still remain in debate, this effect was experimentally observed in group III–V materials such as (In, Mn)As and (Ga, Mn)As.[9–11] However, the electric field controlled ferromagnetism was limited because of the low Curie temperature of (In, Mn)As DMS.[10, 11]

In recent years, Mn doped Si and Ge DMS have attracted extensive attention because of their compatibility with today's Si technology and the possibility to have higher Curie temperatures than those of group III–V materials.[12–23] However, the experimental results show that the Mn doping process in Si and Ge is also complex (even though simpler than group III–V). Both the Curie temperature and the saturation magnetization depend on the interplay of a variety of factors, which are ultimately determined by growth conditions and post-annealing process.[24, 25] The concentration and distribution of Mn dopants, the carrier density, the presence of common defects such as Mn interstitials and Mn clusters significantly influence the magnitude and interactions of the magnetic coupling.[23, 26] It is anticipated that this interplay between various growth parameters can be reduced in low dimensional structures.[27] In addition, nanostructures such as Mn doped Ge quantum dots could offer unique and salient physical properties arising from size and quantum confinement effects, affecting carrier transport, spin lifetimes, and interactions of spins, and thus ferromagnetic properties.[28] More importantly, the magnetic Mn_xGe_{1-x} can be directly incorporated with the current CMOS platforms, promoting immediate applications in the microelectronics industry. Thus in this section, we will describe the progress in the use of nanostructures for this purpose.
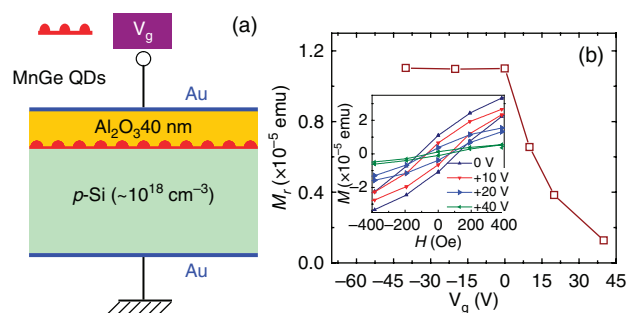
In the past, the research of Mn_xGe_{1-x} nanostructures via Mn ion implantation process has unambiguously demonstrated the modulation of their ferromagnetism by applying gate biases in MOS capacitors at a low temperature of

10 K. However, the metallic precipitates such as Mn_5Ge_3 and $Mn_{11}Ge_8$ and implantation damages were found in these nanostructures, which made the system rather complex to understand the contribution of each phase to the hole mediated effect. In addition, the latter makes it difficult to control the process. A possible approach to eliminate the clusters is to use a self-assembled process, which can yield MnGe quantum dots directly on top of Si substrates. Here, we report the successful development of $Mn_{0.05}Ge_{0.95}$ self-assembled quantum dots by molecular beam epitaxy below.

MnGe quantum dots were grown on *p*-type Si substrates by a solid-source MBE system. The Mn and Ge sources were provided by traditional effusion cells. The self-assembled MnGe quantum dots were developed on the Si surface, similar to the growth of pure Ge quantum dots on Si under a typical Stranski-Krastanow (SK) mode.[29] Cross-section TEM was carried out to determine the structural characteristics and the Mn composition of the $Mn_{0.05}Ge_{0.95}$ quantum dots. It reveals a dome-shape MnGe quantum dot on top of the Si substrate with a Mn diffusion area underneath as shown in Figure 2(a). The dots have a typical base diameter of about 30 nm and a height of about 8 nm. Electron energy loss spectroscopy (EELS) shows that Mn dopants distribute uniformly inside the quantum dots (Fig. 2(b)). The reddish dots represent Mn atoms. The selected area electron diffraction pattern (SAED) reveals a single-crystalline DMS system (Fig. 2(c)). The interface between the dot and the Si substrate shows excellent lattice

Fig. 3. (a) A schematic drawing of a MOS capacitor using MnGe QDs as the channel layer. During the device operation, the gate was applied with positive and negative biases while the magnetic properties were measured by SQUID; (b) Remnant moments as a function of gate voltage at 50 K.

coherence without any pronounced dislocations or stacking faults (Fig. 2(e)). The energy dispersive X-ray spectroscopy (EDS) further confirms the presence of Mn and Ge inside the MnGe quantum dots.

Metal-oxide-semiconductor capacitors using $Mn_{0.05}Ge_{0.95}$ quantum dots as the channel were fabricated and characterized. Figure 3(a) shows a schematic drawing of the device structure. Similar to that of the implanted cased, a 40 nm-thick Al_2O_3 was used to minimize the leakage current. Capacitance–voltage curves show a clear transition from an accumulation (of holes) mode under negative bias to a depletion mode under positive bias (not shown here). Significantly, in the depletion mode we observed the decrease of the ferromagnetism of the channel layer via the control of gate voltage at 50 K (Fig. 3(b)). The remnant moments decrease dramatically as the increase of the gate bias. These experimental data suggest that holes play a significant role in controlling ferromagnetism. By changing the hole concentration in quantum dots, it is possible to manipulate the ferromagnetism in the MnGe DMS system.

4. LOGIC DEVICES WITH SPIN WAVE BUS

For metallic ferromagnetism, one example of using collective phenomena is to use spin wave as a state variable for logic application. Spin wave is a collective oscillation of spins in an ordered spin lattice, which has been studied for decades in a variety of magnetic materials and nanostructures.[30–34] The near-neighbor spins in the lattice are connected via the exchange interaction. Potentially, it is possible to use ferromagnetic films as a conduit for spin wave propagation, referred to as "Spin Wave Bus,"[35] where the information can be coded into a phase or the amplitude of the spin wave as a state variable. The distinct feature and key advantage of the spin wave bus is that information transmission is accomplished without electron transport.

There are several physical properties, which make spin wave utilization promising in magnetic logic circuits. (i) Spin wave, as a highly correlated system of spins, with

Fig. 2. The structural properties of $Mn_{0.05}Ge_{0.95}$ quantum dots grown on a *p*-type Si substrate. (a) a high-resolution TEM cross-section image of a $Mn_{0.05}Ge_{0.95}$ quantum dot. Mn diffuses into the Si substrate, which is shown directly underneath the $Mn_{0.05}Ge_{0.95}$ quantum dot; (b) the EELS composition mapping of Mn distribution; (c) the corresponding SAED pattern of $Mn_{0.05}Ge_{0.95}$ quantum dot, revealing a single crystalline structure; (d) an EDX composition spectrum showing that both Mn and Ge are present in $Mn_{0.05}Ge_{0.95}$ quantum dot. (e) an enlarged HR-TEM image to show the detailed lattice structure of $Mn_{0.05}Ge_{0.95}$ quantum dot.

a long *coherence length*. As it was experimentally demonstrated in spin wave Mach–Zehnder-type interferometer, spin wave signals remain coherent after propagation of millimeters distance in yttrium iron garnet film.[36] In the permalloy films,[32] the coherence length is of the order of tens of microns at *room temperature*. (ii) There is a convenient *mechanism for spin wave to electric signal conversion and vice versa*. Spin wave can be excited by a local magnetic field (e.g., microstrip). A propagating spin wave changes the local polarization of spins in ferromagnetic material, which produces an inductive voltage in a conducting contour. In the experimental works,[30–32] the time-resolved inductive voltage measurement technique has been applied to study propagating spin waves in thin ferromagnetic films. An inductive voltage signal of the order of several mV was detected from spin waves propagated distances up to 50 microns in permalloy ($Ni_{81}Fe_{19}$) film at room temperature.[32] Earlier, spin-wave based logic circuit has been experimentally demonstrated by Kostylev et al.[36] The authors built a spin wave Mach–Zehnder interferometer, which consists of a spin wave generator, a splitter that divides the input spin wave pulses into two ferrite channels made of Yttrium–Iron-Garnet (YIG), two controllable phase shifters attached to the branches, and a mixer where the signals modified by the phase shifter. The phases of the propagating spin waves are controlled by the magnetic fields produced by electric currents in the conducting wires under the waveguides. Depending on the phase shift, the device can operate as NOT or XOR logic gate. The same group has also demonstrated exclusive-not-OR and not-AND gates based on a similar Mach–Zehnder-type spin-wave interferometer structure.[37]

Another prototype spin wave logic device has been recently realized by our group.[38] In Figure 4(a), we show the general view of the device. The core of the structure from the bottom to the top consists of a silicon substrate, a $Co_{30}Fe_{70}$ 100 nm thick film, and a 300 nm thick silicon dioxide layer. There are three asymmetric coplanar strip (ACPS) transmission lines on the top of the structure. The edge ACPS lines are the transducers to excite spin waves, and the line in the center is the receiver to detect the inductive voltage produced by two spin wave signals. The distance between the microstrips is 4 μm. In Figure 4(b), it is shown the experimental data on the output inductive voltage measured at the central ACPS line at different values of the external magnetic field (excitation frequency 3 GHz). The red and black curves depict the output power for the in-phase ($\Delta\phi = 0$) and the out-of-phase ($\Delta\phi = \pi$) cases, respectively. The initial phase difference between two input signals is defined by the direction of the current flow in the excitation lines. The phase difference is zero if the direction of current flow is the same (clockwise or counter-clockwise wise) in both lines. If the directions in the excitation lines are such as one loop is clockwise and the other is counter-clockwise, the spin wave signals receive a π
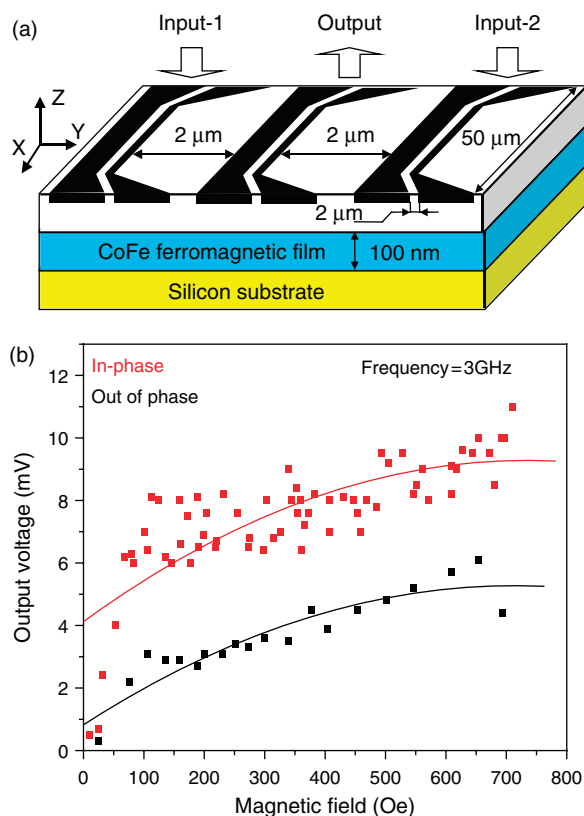

Fig. 4. (a) The general view of the three-terminal spin-wave logic device. The ocre of the structure from the bottom to the top consists of a silicon substrate, a 100-nm-thick CoFe film, and a 300-nm-thick silicon dioxide layer. The three ACPS lines on the top are used as the two input (edge) and one output (in the middle) ports. (b) Experimental data. Output signal amplitude for two spin waves coming in-phase (red curve) and out-of-phase (black curve).

relative phase difference. These experimental data show a prominent (about 4 times) output power difference. All measurements are carried out at *room temperature*.

The main technological problem delaying the practical implementation of spin wave devices is the low excitation efficiency. In all experimentally demonstrated spin wave devices,[36–38] spin wave excitation is via the magnetic field produced by the electric current in the external conducting contours. Equally important, the use of electric current results in the significant energy overhead as the energy for spin wave excitation exceeds the energy of the spin wave by one or two orders of magnitude. In order to realize electric-field controlled spin wave logic devices practical, there should be another physical mechanisms. Multiferroics is a special type of materials that possesses simultaneously electric and magnetic orders,[39,40] the coupling between the electric and magnetic properties provides the unique opportunity to control its magnetic polarization by applied electric field. With recent advent of multiferroic materials, there is a potential for electric field controlled spin wave bus for logic and information processing. A possible solution is in the

use of the multiferroic materials as suggested in Ref. [41]. There are only a few room temperature multiferroic materials known today,[40] e.g., $BiFeO_3$ and its derivatives. An alternative method for obtaining artificial structure with magnetoelectric effect is to couple between two materials such as a ferromagnetic and a ferroelectric.[42] The magnetoelectric coupling may arise as a combined effect of two: piezoelectricity and piezomagnetism. There are several piezoelectric-ferromagnetic pairs, which have been experimentally studied, showing a prominent magnetoelectric coupling: $PZT/NiFe_2O_4$ (1,400 mV cm^{-1} Oe^{-1}),[43] $CoFe_2O_4/BaTiO_3$ (50 mV cm^{-1} Oe^{-1}),[44] $PZT/Terfenol$-D (4,800 mV cm^{-1} Oe^{-1}).[45]

The combination of the multiferroic element with spin wave bus can be also used for spin wave amplification.[46] In Figure 5, we show schematically the material structure of the spin wave device with a magnetoelectric amplifier. From the bottom to the top, it consists of a semiconductor substrate (e.g., silicon), a conducting ferromagnetic film (e.g., CoFe), and a piezoelectric layer (e.g., PZT). The ferromagnetic film serves as a spin wave bus. The metallic contact on the top of the piezoelectric layer and the
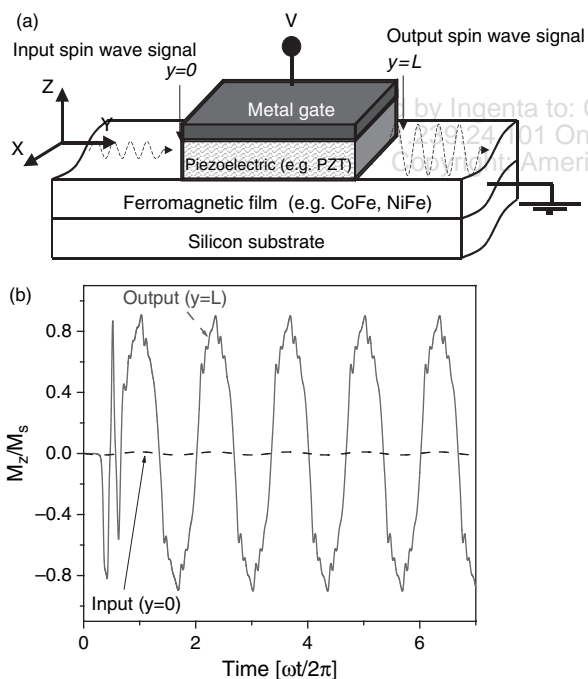
Fig. 5. (a) Schematics of the spin-wave amplifier utilizing the combination with a multiferroic element. From bottom to top, it consists of a semiconductor substrate (e.g., silicon), a conducting ferromagnetic film (e.g., CoFe), and a piezoelectric layer (e. g., PZT). The ferromagnetic film serves as a waveguide for spin waves. The amplitude of the propagating spin wave is amplified in the region under the piezoelectric layer via magnetoelectric coupling. (b) Results of numerical simulations illustrating the time evolution of the normalized magnetization M/Ms. The dashed line depicts the input magnetization at $y = 0$ and solid line depicts the magnetization after amplification at $y = L$. The amplitude of the spin wave is shown to increase as it propagates in the channel under the piezoelectric layer within ($0 < y < L$).
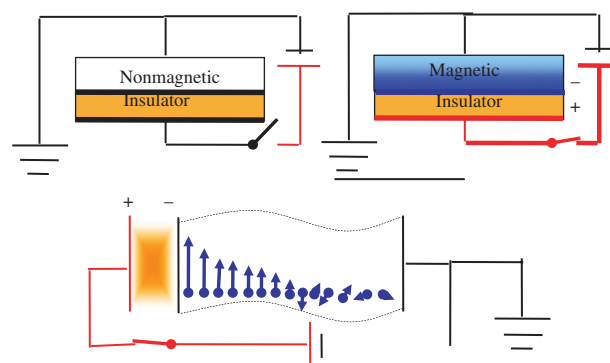
Fig. 6. The two upper figures illustrate that the application of voltage triggers the magnetization across the metallic ferromagnetic film, close to its transition point. Lower figure is an illustration of the "inverse domino" alignment of spins due to the large spin-correlation radius in the critical system, which is near its ferromagnet-paramagnet transition point.

conducting ferromagnetic film (ground plane) serve as a set of two electrodes to apply voltage across the piezoelectric layer. Under the applied bias V, the piezoelectric layer produces pressure, which changes the orientation of the easy-axis in the ferromagnetic film. In turn, the rotation of the easy-axis affects the propagation of the spin wave and can be used for amplification. The results of numerical modeling shown in Figure 5(b), illustrates the increase of the spin wave amplitude as a result of the magnetoelectric coupling. According to the theoretical estimates,[46] the efficiency of the energy conversion using multiferroic element can as high as 97%. The use of magnetoelectric structure in combination with spin wave bus may lead to the development of low-power dissipating magnetic logic devices with functional throughput beyond the capabilities of the scaled CMOS.

5. OUTLOOK ON ELECTRICAL FIELD CONTROL OF METALLIC FERROMAGNETIC MATERIALS

Because of several important technological limitations described above (e.g., power consumption, fluctuations, and cost in fabrication), the most attractive controllable ferromagnetism is that of metals. Metal Spintronics switch if controllable by electric field is ideal and superior to today's semiconductor counter-part for next generations of integrated circuits beyond CMOS. However, in accordance with the Maxwell's magneto-electrodynamics, the electric field can penetrate into a metal only within the surface atomic layer and the conventional wisdom suggests that the external electric control of ferromagnetism in metals is not possible (at least on lengths larger than the lattice constant) in contrast with semiconductors, which let electric field in on much wider depths. In result, metals were excluded from the list of possible candidates for an electric-field-controllable ferromagnetism. The search for

RESEARCH ARTICLE

the controllable ferromagnetism has been focused only on the semiconductor ferromagnets as described above.

Recently, a detailed analysis of the influence of the injected changes on a surface atomic layer of a ferromagnetic metallic film led to the surprising conclusion, opposite to the common knowledge's reasoning. It turned out that the influence of an injected charge on the magnetization is actually more pronounced in metallic ferromagnetic films[47] than in those of semiconductors. This situation appears near the point of a transition between the magnetic and paramagnetic states and is due to the separation on the spatial scale of the "spin"- and "charge"-degrees of freedom in the metallic electron system. As a result, charging a surface affects the spin-alignment (and the existence of the magnetization) across the entire film. The described effect can be thought of as an "inverse domino effect" of exchange interactions between spins of neighboring atoms,[48] consecutively aligning the spins into a magnetization across the entire film. Therefore, the electrically controlled "magnetic switch" can be metallic. Thus, the electrically controlled "magnetic switch" can be metallic.

Metal Spintronics switches are ideal and superior to today's semiconductor counter part for the next generations of integrated circuits beyond CMOS. This finding is especially significant in the light of the fact that because of the high electron density and high conductivity, metals, as compared with semiconductors (including dilute magnetic semiconductors), can be scaled down to much smaller feature sizes and can be stacked in 3 dimensions easily to achieve high integration density as well as to have excellent performance in reducing power dissipation and increasing power variability of today's electronics. The prediction was made only theoretically and if proven experimentally will mostly likely push the limit of the future computational devices further to the horizon, making nonvolatile computers possible.

6. SUMMARY

In summary, we showed that collective effects may be used as state variables for scaled room temperature information processing. The collective state variables seem to have the benefits of lower variability and high efficiency in energy needed for performing computing. For room temperature operation, the collective effect state variables are the choice, in particular, the use of collections of spins as nanomagnets. For single charge electronics, it was shown that the quantum fluctuation will dictate and result in the variability limit due to the large Coulomb interaction energy. On the other hand, for single spin, thermal energy is much higher than the energy of single particle systems at room temperature, i.e., Zeeman splitting, rendering room temperature operation unlikely. We also introduced the spin wave bus concept to illustrate a potential of using collective spins for constructing logic devices and circuits.

References and Notes

1. G. E. Moore, *Electronics* 38, 114 (**1965**).
2. S. A. Wolf, D. D. Awschalom, R. A. Buhrman, J. M. Daughton, S. von Molnar, M. L. Roukes, A. Y. Chtchelkanova, and D. M. Treger, *Science* 294, 1488 (**2001**).
3. I. V. Ovchinnikov and K. L. Wang, *Appl. Phys. Lett.* 92, 093503 (**2008**).
4. D. E. Nikonov and G. I. Bourianoff, *J. Supercond. Nov. Magn.* 21, 479 (**2008**).
5. Y. Ono, Y. Takahashi, K. Yamazaki, M. Nagase, H. Namatsu, K. Kurihara, and K. Murase, Si complementary single-electron inverter, *International Electron Devices Meeting 1999*. Technical Digest (Cat. No.99CH36318). IEEE, Piscataway, NJ, USA (**1999**), pp. 367–70.
6. T. Dietl, H. Ohno, F. Matsukura, J. Cibert, and D. Ferrand, *Science* 287, 1019 (**2000**).
7. F. Matsukura, H. Ohno, A. Shen, and Y. Sugawara, *Phys. Rev. B-Condensed Matter* 57, R2037 (**1998**).
8. M. Yagi, K. Noba, and Y. Kayanuma, *J. Luminescence* 94–95, 523 (**2001**).
9. H. Ohno, D. Chiba, F. Matsukura, T. Omiya, E. Abe, T. Dietl, Y. Ohno, and K. Ohtani, *Nature* 408, 944 (**2000**).
10. D. Chiba, M. Yamanouchi, E. Matsukura, E. Abe, Y. Ohno, K. Ohtani, and H. Ohno, *J. Superconductivity* 16, 179 (**2003**).
11. R. C. Myers, B. L. Sheu, A. W. Jackson, A. C. Gossard, P. Schiffer, N. Samarth, and D. D. Awschalom, *Phys. Rev. B (Condensed Matter and Materials Physics)* 74, 155203 (**2006**).
12. M. Bolduc, C. Awo-Affouda, A. Stollenwerk, M. B. Huang, F. G. Ramos, G. Agnello, and V. P. LaBella, *Phys. Rev. B (Condensed Matter and Materials Physics)* 71, 33302 (**2005**).
13. Y. D. Park, A. T. Hanbicki, S. C. Erwin, C. S. Hellberg, J. M. Sullivan, J. E. Mattson, T. F. Ambrose, A. Wilson, G. Spanos, and B. T. Jonker, *Science* 295, 651 (**2002**).
14. J. S. Kang, G. Kim, S. C. Wi, S. S. Lee, S. Choi, C. Sunglae, S. W. Han, K. H. Kim, H. J. Song, H. J. Shin, A. Sekiyama, S. Kasai, S. Suga, and B. I. Min, *Phys. Rev. Lett.* 94, 147202 (**2005**).
15. M. Passacantando, L. Ottaviano, F. D'Orazio, F. Lucari, M. De Biase, G. Impellizzeri, and F. Priolo, *Phys. Rev. B (Condensed Matter and Materials Physics)* 73, 195207 (**2006**).
16. N. Pinto, L. Morresi, M. Ficcadent, R. Murri, F. D'Orazio, F. Lucari, L. Boarino, and G. Amato, *Phys. Rev. B: Condens. Matter.* 72, 165203 (**2005**).
17. W. Yong, Z. Jin, Z. Zuoming, H. Xinhai, Z. Xiaoyu, and K. L. Wang, *J. Appl. Phys.* 103, 066104 (**2008**).
18. W. Yong, Z. Jin, Z. Zuoming, H. Xinhai, Z. Xiaoyu, and K. L. Wang, *Appl. Phys. Lett.* 92, 101913 (**2008**).
19. Z. Changgan, Z. Wenguang, S. C. Erwin, Z. Zhenyu, and H. H. Weitering, *Phys. Rev. B (Condensed Matter and Materials Physics)* 70, 205340-1-8 (**2004**).
20. A. P. Li, J. F. Wendelken, and J. Shen, *Phys. Rev. B: Condens. Matter.* 72, 195205 (**2005**).
21. S. Ahlers, D. Bougeard, N. Sircar, G. Abstreiter, A. Trampert, M. Opel, and R. Gross, *Phys. Rev. B (Condensed Matter and Materials Physics)* 74, 214411 (**2006**).
22. C. Bihler, C. Jaeger, T. Vallaitis, M. Gjukic, M. S. Brandt, E. Pippel, J. Woltersdorf, and U. Gosele, *Appl. Phys. Lett.* 88, 112506 (**2006**).

23. P. De Padova, J. P. Ayoub, I. Berbezier, P. Perfetti, C. Quaresima, A. M. Testa, D. Fiorani, B. Olivieri, J. M. Mariot, A. Taleb-Ibrahimi, M. C. Richter, O. Heckmann, and K. Hricovini, *Phys. Rev. B (Condensed Matter and Materials Physics)* 77, 045203 (**2008**).

24. M. Bolduc, C. Awo-Affouda, F. Ramos, and V. P. LaBella, *J. Vacuum Sci. Tech. A (Vacuum, Surfaces, and Films)* 24, 1648 (**2006**).

25. M. Jamet, A. Barski, T. Devillers, V. Poydenot, R. Dujardin, P. Bayle-Guillemaud, J. Rothman, E. Bellet-Almaric, A. Marty, J. Cibert, R. Mattana, and S. Tatarenko, *Nature Materials* 5, 653 (**2006**).

26. E. Biegger, L. Staheli, M. Fonin, U. Rudiger, and S. Dedkov Yu, *J. Appl. Phys.* 101, 103912 (**2007**).

27. K. Brunner, *Reports on Progress Phys.* 65, 27 (**2002**).

28. R. Knobel, N. Samarth, S. A. Crooker, and D. D. Awschalom, *Physica E* 6, 786 **2000**.

29. J. L. Liu, S. Tong, and K. L. Wang, Self-assembled Ge quantum dots on Si and their optoelectronic devices, Handbook of Semiconductor Nanostructure and Devices, edited by A. A. Balandin and K. L. Wang (**2006**), Vol. 1, pp. 1–32.

30. T. J. Silva, C. S. Lee, T. M. Crawford, and C. T. Rogers, *J. Appl. Phys.* 85, 7849 (**1999**).

31. B. A. Kalinikos, N. G. Kovshikov, M. P. Kostylev, P. Kabos, and C. E. Patton, *JETP Lett.* 66, 371 (**1997**).

32. M. Covington, T. M. Crawford, and G. J. Parker, *Phys. Rev. Lett.* 89, 237202 (**2002**).

33. M. Bailleul, D. Olligs, C. Fermon, and S. Demokritov, *Europhysics Lett.* 56, 741 (**2001**).

34. M. Bailleul, R. Hollinger, and C. Fermon, *Phys. Rev. B (Condensed Matter and Materials Physics)* 73, 104424 (**2006**).

35. A. Khitun and K. Wang, *Superlattices and Microstructures* 38, 184 (**2005**).

36. M. P. Kostylev, A. A. Serga, T. Schneider, B. Leven, and B. Hillebrands, *Appl. Phys. Lett.* 87, 153501 (**2005**).

37. T. Schneider, A. A. Serga, B. Leven, B. Hillebrands, R. L. Stamps, and M. P. Kostylev, *Appl. Phys. Lett.* 92, 022505 (**2008**).

38. A. Khitun, M. Bao, Y. Wu, J.-Y. Kim, A. Hong, A. Jacob, K. Galatsis, and K. L. Wang, *Mater. Res. Soc. Symp. Proceedings* 1067, B01 (**2008**).

39. G. A. Smolenskii and I. E. Chupis, *Soviet Physics-Uspekhi* 25, 475 (**1982**).

40. H. Zheng, J. Wang, S. E. Lofland, Z. Ma, L. Mohaddes-Ardabili, T. Zhao, L. Salamanca-Riba, S. R. Shinde, S. B. Ogale, F. Bai, D. Viehland, Y. Jia, D. G. Schlom, M. Wuttig, A. Roytburd, and R. Ramesh, *Science* 303, 661 (**2004**).

41. A. Khitun, M. Bao, and K. L. Wang, *IEEE Trans. on Magnetics* 44, 2141 (**2008**).

42. W. Eerenstein, N. D. Mathur, and J. F. Scott, *Nature* 442, 759 (**2006**).

43. G. Srinivasan, E. T. Rasmussen, J. Gallegos, R. Srinivasan, I. Bokhan Yu, and V. M. Laletin, *Phys. Rev. B (Condensed Matter and Materials Physics)* 64, 2144081 (**2001**).

44. J. Van Den Boomgaard, D. R. Terrell, R. A. J. Born, and H. Giller, *J. Mater. Sci.* 9, 1705 (**1974**).

45. R. Jungho, V. Carazo, K. Uchino, and K. Hyoun-Ee, *Japanese J. Appl. Phys. Part 1 (Regular Papers, Short Notes and Review Papers)* 40, 4948 (**2001**).

46. A. Khitun, D. E. Nikonov, and K. L. Wang, *J. Appl. Phys.* 106, 123909 (**2009**).

47. I. V. Ovchinnikov and K. L. Wang, *Phys. Rev. B* 80, 012405 (**2009**).

48. I. V. Ovchinnikov and K. L. Wang, *Phys. Rev. B (Condensed Matter and Materials Physics)* 79, 020402 (**2009**).

RESEARCH ARTICLE